

Potential theory and analytic properties of a Cantor set

C P Dettmann and N E Frankel

School of Physics, University of Melbourne, Parkville, Victoria 3052, Australia

Received 4 August 1992, in final form 20 November 1992

Abstract. We consider the electrostatic potential due to a uniform distribution of charge on a Cantor set. Mellin transforms are used to find expansions for the potential at a distance r from the end of the charge distribution. It is found that the potential is a power law multiplied by a function periodic in $\ln r$, together with a power series in r . A recursion relation for the moments of the distribution is used to reveal a similar structure in these moments. Finally Fourier transform techniques are used to find explicit representations for the distribution and its moments.

1. Introduction

Fractals play an important role in modelling many physical systems. Whether as a result of nonlinear dynamics (to give some examples from a vast literature: chaotic attractors [1], turbulence [2], the rings of Saturn [3], and even quantum mechanics [4]) or random processes (for example Brownian motion [5] or diffusion limited aggregation—DLA [6]) most of the analyses have been numerical in nature, with analytical sections limited to proving the existence of fractal behaviour, and perhaps calculating a small number of useful parameters, such as dimensions. The main exception is the work of Bessis *et al* [7], who investigated Mellin transforms and various analytic properties of Julia sets, fractals generated by a single nonlinear transformation on the complex field. They made extensive use of functional equations and found that the Mellin transform of the fractal distribution is a meromorphic function with a semi-infinite periodic array of poles, in addition to other interesting analytic properties. These results need to be generalized since many important fractals are of higher dimension than that of Julia sets (two) and/or require more than one transformation to represent them. The methods used in this paper are applicable to fractal distributions generated by more than one transformation, provided that these are similarity transformations.

The problem we are concerned with is solving Laplace's equation with fractal boundary conditions, with the aim of determining as much as possible about the solution using analytical methods, in particular Mellin transforms. While mathematicians have studied the general structure of the potential about singular points [8], there has been virtually no detailed analytical work with application to specific fractals. General scaling laws have been used to calculate the statistical properties, for example fluctuations in intensity, in waves diffracted from a fractal phase-shifting screen [9]. Recently there have been numerical investigations in this area, specifically modes of vibration of a fractal drum [10] and the potential around

a fractal, charged conducting surface as a model for DLA [6]. Both of these studies have found that the solution has a self-similar structure closely related to that of the fractal.

In this paper we consider the potential produced by a uniform charge distribution on a Cantor set, which is one of the classic and most well known exactly self-similar fractals. The insights to be gained from this analysis apply to more complicated self-similar fractal distributions, and should also shed light on problems involving random fractals, for which a complete analysis is more difficult. The potential is closely related to the moments of the distribution (section 3) and the Fourier transform (section 4), both of which show a rich analytic structure.

2. Potential from a Cantor set

The ‘middle third Cantor set’ is defined by an iterative process. Beginning with a line segment, which we specify as $(-1/2, 1/2)$ on the x -axis, the middle of the segment is removed, leaving two segments each of which is one-third of the original length. Then the process is repeated on each of these segments, and so on. The Cantor set is the set of points remaining. See figure 1. The question of whether the segments are open or closed is irrelevant for the purposes of this paper, since these endpoints constitute only a countable set, while the remaining points form an uncountable set.

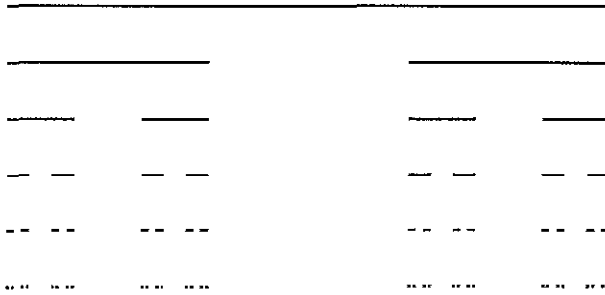


Figure 1. The construction of the Cantor set. The ends of the line segment shown are taken to have coordinates $(-1/2, 0)$ and $(1/2, 0)$.

There are a number of different definitions of the dimension of a set. The topological dimension of the Cantor set is zero, as it consists of disconnected points. The Euclidean dimension of the space in which it is embedded is one. See Mandelbrot [11]. Both of these dimensions are always integers, but there are a number of definitions which allow non-integral dimensions. Among these are the Hausdorff and box-counting dimensions, both of which are defined in Falconer [12], and both of which give

$$d = \ln 2 / \ln 3 \tag{2.1}$$

for the Cantor set. It is well known that for a point, line and plane of charge the electrostatic potential is given by

$$V \sim r^{d-1} \tag{2.2}$$

in the limit $r \rightarrow 0$, where r is the distance from the charge and d is the dimension of the charge distribution. A dependence of r^0 is taken to be equivalent to $\ln r$. The question then arises: Does this result generalize to the situation of non-integer dimension? We find that the simple power law does not hold exactly, for reasons that will become clear in the following analysis.

The great advantage in working with an exactly self-similar set such as the Cantor set is that the definition of a uniform charge distribution is unambiguous—it is the only distribution for which the charge on identical regions of the set are equal. This uniqueness is used to maximum advantage in defining the charge distribution $C(x)$ by

$$C(x) = \frac{3}{2}[C(3x - 1) + C(3x + 1)] \tag{2.3}$$

with normalization

$$\int_{-\infty}^{\infty} C(x) dx = 1. \tag{2.4}$$

This distribution is similar to the Dirac distribution in that it is ‘infinite’ at all points in the Cantor set, and ‘zero’ elsewhere. The factor $3/2$ is necessary for a consistent normalization. All the properties of the charge distribution may be obtained from equations (2.3) and (2.4). Mandelbrot [11] has made the point that the Hausdorff measure may be used to define the concept of a uniform distribution when self-similarity is not exact, but this may be of limited use in realistic situations due to the difficulty of calculating the Hausdorff measure in most cases.

The potential due to this distribution in the x - y plane may be determined by the usual integral, which in suitable units becomes

$$V(x, y) = \int_{-\infty}^{\infty} \frac{C(x') dx'}{\sqrt{(x - x')^2 + y^2}} = V(-x, y). \tag{2.5}$$

The remainder of this section discusses the means of calculation, and analytic properties of the above integral. The integrand is expanded in a power series in x' to obtain

$$V(x, y) = \sum_{n=0}^{\infty} \frac{C_n}{n!} \frac{\partial^n}{\partial x'^n} \frac{1}{\sqrt{(x - x')^2 + y^2}} \Big|_{x'=0} \tag{2.6}$$

where

$$C_n = \int_{-\infty}^{\infty} C(x) x^n dx. \tag{2.7}$$

The calculation and asymptotic properties of the C_n are interesting in their own right, and are discussed fully in the next section, which may be read independently of this section.

Substituting equation (2.3) into equation (2.5) yields

$$V(x, y) = \frac{3}{2}[V(3x - 1, 3y) + V(3x + 1, 3y)] \tag{2.8}$$

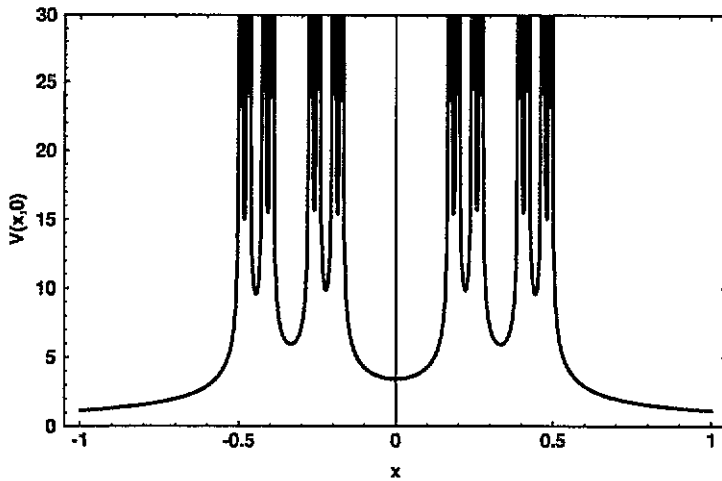


Figure 2. The potential of the Cantor set along the line $y = 0$.

which, by repeated application, may be used to write the potential near the fractal in terms of the potential further away, so that the series (2.6) which converges rapidly for $\sqrt{x^2 + y^2} > 1$, may be used to numerically evaluate $V(x, y)$ at all points not on the fractal. In this way figure 2 was generated. The authors have also plotted a three-dimensional graph of $V(x, y)$ in the whole x - y plane [13].

Now we consider the potential near the edge of the fractal at $(1/2, 0)$. Using equation (2.8) we obtain

$$V(x + \frac{1}{2}, y) = \frac{3}{2}[V(3x + \frac{1}{2}, 3y) + V(3x + \frac{5}{2}, 3y)]. \tag{2.9}$$

The point $(3x + 1/2, 3y)$ is still near the fractal if x and y are small. So the first term on the right-hand side is substituted back into equation (2.8). This process is continued indefinitely, to obtain

$$V(x + \frac{1}{2}, y) = \sum_{j=1}^{\infty} \left(\frac{3}{2}\right)^j V(3^j x + \frac{5}{2}, 3^j y). \tag{2.10}$$

At this point there is a simple argument to show that equation (2.2) holds, at least approximately, for the line $y = 0$. The maximum term in the above series occurs when $3^j x$ is of order 1, that is

$$j_{\max} = -\ln x / \ln 3. \tag{2.11}$$

For $j > j_{\max}$ the terms decrease exponentially, since $V(x, y) \sim (x^2 + y^2)^{-1/2}$ at large distances. The maximum term is equal to $V(3^{j_{\max}} x + 5/2)$, which is a number of order 1, multiplied by $(3/2)^{j_{\max}}$. Thus

$$V(x + \frac{1}{2}, 0) \sim \left(\frac{3}{2}\right)^{j_{\max}} = x^{\ln 2 / \ln 3 - 1}. \tag{2.12}$$

Now we proceed with an exact calculation which obtains not only the coefficient of x^{d-1} , but also the correction terms to it. Substituting equation (2.6) into

equation (2.10) and rearranging sums we obtain

$$V(x + \frac{1}{2}, y) = \sum_{n=0}^{\infty} \frac{C_n}{n!} \sum_{j=1}^{\infty} \left(\frac{3}{2}\right)^j \frac{\partial^n}{\partial x'^n} \frac{1}{\sqrt{(3^j x - x' + 5/2)^2 + (3^j y)^2}} \Big|_{x'=0}. \quad (2.13)$$

This expression is fairly complicated to evaluate, so we restrict our treatment to two limits. Firstly along the line $y = 0$ the derivative may be performed explicitly to obtain

$$V(x + \frac{1}{2}, 0) = \sum_{n=0}^{\infty} \frac{C_n}{n!} \sum_{j=1}^{\infty} \left(\frac{3}{2}\right)^j \frac{n!}{(3^j x + 5/2)^{n+1}} \quad (2.14)$$

and the summand is Mellin transformed [14] with x as the transformed variable, so that the sum over j becomes a geometric series. The result is

$$V(x + \frac{1}{2}, 0) = \sum_{n=0}^{\infty} \frac{C_n}{n!} \left(\frac{2}{5}\right)^{n+1} \frac{1}{2\pi i} \int_{c-i\infty}^{c+i\infty} \frac{\Gamma(s)\Gamma(n+1-s)}{2.3^{s-1} - 1} \left(\frac{2x}{5}\right)^{-s} ds \quad (2.15)$$

with

$$1 - \frac{\ln 2}{\ln 3} < c < 1. \quad (2.16)$$

The gamma function $\Gamma(z)$ has a pole of residue $(-1)^p/p!$ at $z = -p$ for all non-negative integers p . In addition there is a set of poles arising from the denominator, of residue $1/\ln 3$ at $s = 1 - \ln 2/\ln 3 + 2\pi im/\ln 3$ for all integers m . Thus closing the contour in (2.15) to the left, we obtain

$$\begin{aligned} V(x + \frac{1}{2}, 0) &= \frac{1}{\ln 3} \sum_{n=0}^{\infty} \frac{C_n}{n!} \left(\frac{2}{5}\right)^{n+1} \sum_{m=-\infty}^{\infty} \Gamma(s_m)\Gamma(n+1-s_m) \left(\frac{2x}{5}\right)^{-s_m} \\ &+ \sum_{n=0}^{\infty} \frac{C_n}{n!} \left(\frac{2}{5}\right)^{n+1} \sum_{p=0}^{\infty} \frac{(-1)^p}{p!} \frac{\Gamma(n+1+p)}{2.3^{-p-1} - 1} \left(\frac{2x}{5}\right)^p \end{aligned} \quad (2.17)$$

where

$$s_m = 1 - \frac{\ln 2}{\ln 3} + \frac{2\pi im}{\ln 3}. \quad (2.18)$$

This can be written as

$$V(x + \frac{1}{2}, 0) = \sum_{p=0}^{\infty} a_{x,p} x^{-1+\ln 2/\ln 3} \cos\left(\frac{2\pi p}{\ln 3} \ln x + \phi_{x,p}\right) + b_{x,p} x^p \quad (2.19)$$

and numerical values of the $a_{x,p}$, $b_{x,p}$ and $\phi_{x,p}$ are tabulated in table 1. It can be shown that this series converges for $x \leq 2$. The presence of a vertical infinite sequence of poles is quite characteristic of the Mellin transform of a function with fractal behaviour; this case is quite similar to that of Julia sets [7] and the Weierstrass

Table 1. *X* coefficients. See equation (2.19).

<i>p</i>	<i>a</i> _{<i>x,p</i>}	<i>b</i> _{<i>x,p</i>}	<i>φ</i> _{<i>x,p</i>}
0	1.768 50	-1.224 69	0
1	7.049 77 × 10 ⁻⁸	2.186 60 × 10 ⁻¹	1.592 91
2	6.757 50 × 10 ⁻¹⁷	-7.803 19 × 10 ⁻²	-2.686 66
3	1.157 41 × 10 ⁻²³	3.205 48 × 10 ⁻²	0.631 06
4	1.836 01 × 10 ⁻³¹	-1.386 97 × 10 ⁻²	1.725 81
5	1.193 83 × 10 ⁻³⁹	6.159 87 × 10 ⁻³	2.369 46
6	1.698 14 × 10 ⁻⁴⁷	-2.781 74 × 10 ⁻³	2.322 73

function [15]. Thus the power-law behaviour equation (2.2) is modified by a function periodic in ln *x*, even if most of the Fourier coefficients are rather small (table 1).

Closing the contour to the right generates

$$\begin{aligned}
 V(x + \frac{1}{2}, 0) &= \sum_{n=0}^{\infty} C_n \sum_{p=0}^{\infty} \frac{(n+p)!}{n!p!} \left(\frac{-5}{2}\right)^p \frac{x^{-(1+n+p)}}{2.3^{n+p}-1} \\
 &= \frac{1}{x} - \frac{1}{2x^2} + \frac{3}{8x^3} - \frac{5}{16x^4} + \frac{87}{320x^5} - \dots
 \end{aligned}
 \tag{2.20}$$

which is the same function, expanded for large *x*. It is, in fact, equation (2.6) shifted by 1/2.

Secondly we consider the limit of *x* = 0 in equation (2.13). The derivative cannot be performed explicitly, so we do the Mellin transform first, and then complete the derivative and sum over *j*. After some simplification using the reflection and doubling formulae for the gamma functions, the result is

$$V(\frac{1}{2}, y) = \sum_{n=0}^{\infty} \frac{C_n}{n!} \left(\frac{2}{5}\right)^{n+1} \frac{1}{2\pi i} \int_{c-i\infty}^{c+i\infty} \frac{1}{2.3^{s-1}-1} \frac{\Gamma(n+1-s)\Gamma(s/2)}{2\Gamma(1-s/2)} \left|\frac{y}{5}\right|^{-s} ds
 \tag{2.21}$$

with

$$1 - \frac{\ln 2}{\ln 3} < c < 1
 \tag{2.22}$$

as before. Note that the potential is an even function of *y*, hence the absolute value signs. Closing the contour to the left in the above expression we obtain

$$\begin{aligned}
 V(\frac{1}{2}, y) &= \frac{1}{2 \ln 3} \sum_{n=0}^{\infty} \frac{C_n}{n!} \left(\frac{2}{5}\right)^{n+1} \sum_{m=-\infty}^{\infty} \frac{\Gamma(n+1-s_m)\Gamma(s_m/2)}{\Gamma(1-s_m/2)} \left|\frac{y}{5}\right|^{-s_m} \\
 &\quad + \sum_{n=0}^{\infty} \frac{C_n}{n!} \left(\frac{2}{5}\right)^{n+1} \sum_{p=0}^{\infty} \frac{(-1)^p}{p!} \frac{1}{2.3^{-2p-1}-1} \frac{\Gamma(n+1+2p)}{\Gamma(p+1)} \left|\frac{y}{5}\right|^{2p}
 \end{aligned}
 \tag{2.23}$$

which may be written

$$V(\frac{1}{2}, y) = \sum_{p=0}^{\infty} a_{y,p} |y|^{-1+\ln 2/\ln 3} \cos\left(\frac{2\pi p}{\ln 3} \ln |y| + \phi_{y,p}\right) + b_{y,p} |y|^p.
 \tag{2.24}$$

The $a_{y,p}$, $b_{y,p}$ and $\phi_{y,p}$ are tabulated in table 2. It can be shown that this series converges for $|y| \leq 2$. Note that, although the coefficients of the diverging terms $y^{\ln 2 / \ln 3 - 1}$ are different from the corresponding x coefficients, the constant term is the same for both cases

$$b_{y,0} = b_{x,0} \tag{2.25}$$

as it would be if the potential were finite, since for a finite potential, both expansions start with the value of the potential at the point to be expanded around.

Table 2. Y coefficients. See equation (2.24).

p	$a_{y,p}$	$b_{y,p}$	$\phi_{y,p}$
0	2.064 75	-1.224 69	0
1	$9.392\ 43 \times 10^{-5}$	0	1.398 78
2	$5.068\ 17 \times 10^{-10}$	$3.901\ 60 \times 10^{-2}$	-2.886 58
3	$5.648\ 97 \times 10^{-13}$	0	0.429 22
4	$6.186\ 19 \times 10^{-17}$	-5.20113×10^{-3}	1.523 01
5	$2.868\ 07 \times 10^{-21}$	0	2.166 08
6	$2.968\ 87 \times 10^{-25}$	$8.692\ 94 \times 10^{-4}$	2.118 97

Closing the contour to the right generates the large $|y|$ expansion:

$$\begin{aligned}
 V(\frac{1}{2}, y) &= \sum_{n=0}^{\infty} \frac{C_n}{n!} \left(\frac{2}{5}\right)^{n+1} \sum_{p=0}^{\infty} \frac{(-1)^p}{p!} \frac{\Gamma((1+n+p)/2)}{2\Gamma((1-n-p)/2)} \frac{1}{2 \cdot 3^{n+p} - 1} \left|\frac{y}{5}\right|^{-(1+n+p)} \\
 &= \frac{1}{|y|} - \frac{3}{16|y|^3} + \frac{261}{2560|y|^5} - \dots
 \end{aligned} \tag{2.26}$$

Note that only odd powers of $|y|$ contribute, since the gamma function in the denominator has poles for alternate values of p .

3. Evaluation and asymptotics of the C_n

Now we return to a calculation of the C_n , defined by equation (2.7). Equation (2.3) is substituted into this definition and the binomial expansion is used to put the resulting expression into the same form as equation (2.7), giving the following recursion relation for the C_n

$$C_n = \frac{1}{3^n} \sum_{j=0}^{n/2} \binom{n}{2j} C_{n-2j}. \tag{3.1}$$

These relations separate into two disjoint sets of equations for odd and even n . The equation for C_1 implies that $C_1 = 0$, and it follows that $C_n = 0$ if n is odd. This is apparent from the reflection symmetry of the initial distribution. For even n the

Table 3. The moments of the Cantor distribution and asymptotic coefficients. See equations (3.4), (3.27) and (3.28).

p	C_{2p}	$a_{c,p}$	$\phi_{c,p}$
0	1	0.947 814	0
1	1/8	$3.637\ 88 \times 10^{-4}$	-1.682 90
2	7/320	$3.044\ 36 \times 10^{-9}$	0.664 40
3	205/46 592	$4.383\ 62 \times 10^{-12}$	-1.296 91
4	10 241/10 915 840	$5.756\ 45 \times 10^{-16}$	-2.979 10
5	26 601 785/128 911 704 064	$3.072\ 45 \times 10^{-20}$	0.627 73
6	144 273 569 311/3 114 038 000 353 280	$3.568\ 24 \times 10^{-24}$	-2.509 94

C_n are defined in terms of C_0 , which is given by the normalization, equation (2.4). In summary

$$C_0 = 1 \tag{3.2}$$

$$C_n = 0 \quad \text{for } n \text{ odd} \tag{3.3}$$

$$C_n = \frac{1}{3^n - 1} \sum_{j=0}^{n/2-1} \binom{n}{2j} C_{2j} \quad \text{for } n \geq 2 \text{ and even.} \tag{3.4}$$

The first few values are given in table 3. For larger values of n the exact expressions for C_n rapidly become more complicated, for example the numerator of C_{100} —expressed in simplest form—has 1055 digits, and it is difficult to see from equation (3.4) what the asymptotic behaviour is as $n \rightarrow \infty$. We begin with the following ansatz, based on intuition and preliminary numerical investigation,

$$C_n = a^n n^b f(n) \tag{3.5}$$

where $f(n)$ is a bounded function which, apart from being ‘slowly varying’ ($f'(n)/f(n) \ll 1/\sqrt{n}$), is as yet unspecified. Numerical calculations using equation (3.1) have been done to generate a plot of $f(n)$, using the values of a and b found in equations (3.15) and (3.16) which is given in figure 3.

The contribution from the endpoints of the sum in equation (3.4) is negligible for sufficiently large n , irrespective of the values of a and b , due to the presence of the binomial coefficient. Hence $2j$ and $n - 2j$ are both sufficiently large to use Stirling’s formula

$$p! = p^p e^{-p} \sqrt{2\pi p} [1 + O(1/p)]. \tag{3.6}$$

Thus the summand may be written

$$\binom{n}{2j} C_{2j} = \left(\frac{an}{2j}\right)^{2j} \left(\frac{n}{n-2j}\right)^{n-2j} g(j) \tag{3.7}$$

where

$$g(j) = (2j)^b \sqrt{\frac{n}{2j(n-2j)}} \frac{f(2j)}{\sqrt{2\pi}} \tag{3.8}$$

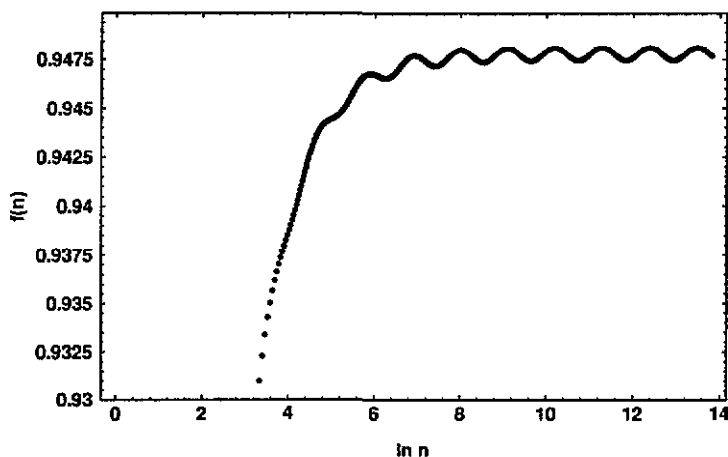


Figure 3. The numerical evaluation of $f(n)$, which appears in the expansion for the C_n . See equation (3.5). The $1/n$ term and the first non-trivial Fourier coefficient are clearly seen.

We assume $g(j)$ is effectively constant over the range of j which contribute. This is valid because this range is of order \sqrt{n} as shown by equation (3.13), while j itself is of order n (see below). Its value will be taken to be at the value of j for which the summand is a maximum

$$j_{\max} = \frac{na}{2(1+a)} \tag{3.9}$$

not to be confused with the j_{\max} of the previous section.

Because the number of terms which contribute is much greater than 1, the sum may be taken to an integral, with the Euler-Maclaurin corrections being negligible to this order,

$$\sum_{j=0}^{n/2-1} \binom{n}{2j} C_{2j} = g(j_{\max}) \int_0^{n/2} \left(\frac{an}{2j}\right)^{2j} \left(\frac{n}{n-2j}\right)^{n-2j} dj \tag{3.10}$$

$$= \frac{n}{2} g(j_{\max}) \int_0^1 \left(\frac{a}{z}\right)^{nz} \left(\frac{1}{1-z}\right)^{n(1-z)} dz \tag{3.11}$$

where

$$z = 2j/n. \tag{3.12}$$

The integrand is written as an exponential and expanded in a Taylor series about its maximum to obtain

$$\frac{n}{2} g(j_{\max}) \int_0^1 \exp \left[n \left(\ln(a+1) - \frac{(a+1)^2}{2a} \left(z - \frac{2j_{\max}}{n} \right)^2 + \dots \right) \right] dz. \tag{3.13}$$

Because the factor of n in the exponential is so large, the above quadratic approximation gives an accurate expression for the integral, leading to

$$C_n = a^n n^b f(n) = \left(\frac{a+1}{3}\right)^n \left(\frac{na}{a+1}\right)^b \frac{a+1}{3\sqrt{2a}} f\left(\frac{n}{3}\right) \tag{3.14}$$

which implies that

$$a = \frac{1}{2} \tag{3.15}$$

$$b = -\frac{\ln 2}{\ln 3} \tag{3.16}$$

$$f(n) = f(n/3). \tag{3.17}$$

The fact that $a = 1/2$ is consistent with the fact that the series, equation (2.6) must diverge at the edge of the fractal $(1/2, 0)$. The value of b is an example of the way that the dimension of the fractal may appear in unexpected places. The function f may be expanded in a Fourier series in $\ln n$, analogous to equation (2.19), multiplied by one plus a function of n which is order $1/n$. See figure 3. Since there is such a close connection between the C_n as $n \rightarrow \infty$ and $V(1/2 + x, 0)$ as $x \rightarrow 0$, and there is a complete expansion for the latter, given in the previous section, it is possible to determine more information about the former, in particular, the coefficients of the Fourier series for $f(n)$. This we proceed to do.

Equation (2.6) gives, in the limit $y \rightarrow 0$,

$$V(x + \frac{1}{2}, 0) = \sum_{n=0}^{\infty} \frac{C_n}{(x + 1/2)^{n+1}} \tag{3.18}$$

which may be written as

$$V(x + \frac{1}{2}, 0) = h(x) + \frac{1}{2} \sum_{n=N}^{\infty} \frac{n^{-\ln 2 / \ln 3} f(n)}{2^n (x + 1/2)^{n+1}} \tag{3.19}$$

where $h(x)$ is a function which tends to a constant as $x \rightarrow 0$, for arbitrarily large N . The factor of $1/2$ comes from the fact that half of the C_n are zero. We will ignore all terms which are finite in the $x \rightarrow 0$ limit, and use a ' \sim ' to denote this. Performing a Mellin transform on the above sum, using x as the transformed variable, we obtain

$$V(x + \frac{1}{2}, 0) \sim \frac{1}{2\pi i} \int_{c-i\infty}^{c+i\infty} (2x)^{-s} \Gamma(s) S(s) ds \tag{3.20}$$

where

$$S(s) = \sum_{n=N}^{\infty} f(n) n^{-\ln 2 / \ln 3} \frac{\Gamma(n + 1 - s)}{\Gamma(n + 1)} \tag{3.21}$$

for

$$1 - \frac{\ln 2}{\ln 3} < c < N + 1. \tag{3.22}$$

The sum $S(s)$ has a set of poles at the s_m defined by equation (2.18). The residue at each of these values may be determined by using the formula

$$\frac{\Gamma(n + 1 - s)}{\Gamma(n + 1)} = n^{-s} (1 + O(s/n)) \tag{3.23}$$

which is easily obtained from Stirling's formula, equation (3.6), and is valid for arbitrary complex s for sufficiently large n . In addition $f(n)$ is written as

$$f(n) = \sum_{p=0}^{\infty} a_{c,p} \cos \left(\frac{2\pi p}{\ln 3} \ln n + \phi_{c,p} \right) \tag{3.24}$$

which is also valid for sufficiently large n . The sum is taken to an integral to obtain

$$S(s) = \int_N^{\infty} n^{-s - \ln 2 / \ln 3} \sum_{p=0}^{\infty} a_{c,p} \cos \left(\frac{2\pi p}{\ln 3} \ln n + \phi_{c,p} \right) dn. \tag{3.25}$$

The variable in the integral is changed to $\ln n$, which puts it into a form which is readily evaluated, to obtain the required residues,

$$\text{Res}_{s=s_m} S(s) = \begin{cases} a_{c,p} e^{i\phi_{c,p}} / 2 & \text{for } m = p > 0 \\ a_{c,0} & \text{for } m = 0 \\ a_{c,p} e^{-i\phi_{c,p}} / 2 & \text{for } m = -p < 0 \end{cases} \tag{3.26}$$

which may be compared with equation (2.19) to give, finally,

$$a_{c,p} = \left| \frac{2^{s_p}}{\Gamma(s_p)} \right| a_{x,p} \tag{3.27}$$

$$\phi_{c,p} = \arg \left(\frac{2^{s_p}}{\Gamma(s_p)} \right) - \phi_{x,p}. \tag{3.28}$$

The $a_{c,p}$ and $\phi_{c,p}$ are tabulated in table 3. It may seem somewhat circular to write the asymptotic form of the C_n in terms of a series of C_n , however this series, equation (2.17) is rapidly convergent, so only the first few terms need to be included in practice.

The full expansion for the C_n includes terms of order $1/n$ and smaller. These could be calculated, in principle, by including extra terms in Stirling's formula, taking account of the variation of $g(j)$, and including the appropriate corrections for the Euler-Maclaurin expansion and the steepest descent calculation.

4. Fourier transform of the Cantor set

One of the features of self-similar structures is that the dimensionality of the structure appears in the power spectrum. The Fourier transform has obvious applications in treating the diffraction patterns from fractal objects. See Berry [9] and references therein for more on this subject. In addition, many functions are better represented as Fourier series or integrals than the corresponding power series. In this section we give analytical results relating to the Fourier transform of the Cantor distribution, $\tilde{C}(k)$, defined by

$$\tilde{C}(k) = \int e^{ikx} C(x) dx. \tag{4.1}$$

This can be evaluated numerically for small k by expanding the exponential in a power series, resulting in

$$\tilde{C}(k) = \sum_{n=0}^{\infty} \frac{C_n}{n!} (ik)^n \quad (4.2)$$

which converges rapidly if k is not too large. A more useful approach is to substitute the recursion relation for $C(x)$, equation (2.3) into equation (4.1) directly, which gives

$$\tilde{C}(k) = \cos(k/3) \tilde{C}(k/3) \quad (4.3)$$

which can be used to obtain the remarkably simple explicit expression

$$\tilde{C}(k) = \prod_{j=1}^{\infty} \cos(3^{-j} k). \quad (4.4)$$

The above expression was obtained by Hille and Tamarkin [16], and the treatment given here will be correspondingly brief. The form of the product makes sense intuitively, since the Cantor set may be regarded as the convolution of an infinite number of double spikes of appropriate separations. The product converges for all values of k , indicating that the result is an entire function of k . The graph of $\tilde{C}(k)$ is given in figure 4, and was obtained by a combination of equations (4.2) and (4.3). Thus we have an integral representation for the Cantor distribution

$$C(x) = \int_{-\infty}^{\infty} \frac{dk}{2\pi} e^{-ikx} \prod_{j=1}^{\infty} \cos(3^{-j} k) \quad (4.5)$$

and, using equation (4.2), an explicit representation for the Cantor moments,

$$C_n = (-i)^n \left. \frac{d^n}{dk^n} \prod_{j=1}^{\infty} \cos(3^{-j} k) \right|_{k=0}. \quad (4.6)$$

Returning to $\tilde{C}(k)$, it can be seen from equation (4.4) that if k is an odd multiple of $3\pi/2$, at least one of the terms in the product is zero, while if it is an even multiple of $3\pi/2$, at least one of the terms in the product has magnitude one. The outcome of these considerations is the presence of a hierarchy of multiple zeros in the first case, and the fact that for arbitrarily large values of k , specifically for $k = 3^j \pi$, $\tilde{C}(k)$ is given by $\tilde{C}(\pi)$, which is $0.466275\dots$ in the second case. Thus when we discuss the behaviour as $k \rightarrow \infty$, it is only in some average sense, as this limit is not well defined.

If we consider the expression for $[\tilde{C}(k)]^2$, terminating the product when the argument of the cosine is of order one, and using the geometric mean of the \cos^2 function

$$\exp\left(\frac{2}{\pi} \int_0^{\pi/2} \ln \cos^2 x \, dx\right) = \frac{1}{4} \quad (4.7)$$

for the remaining terms, we obtain

$$[\tilde{C}(k)]^2 \sim k^{-2 \ln 2 / \ln 3} \quad (4.8)$$

which is yet another appearance of the dimension of the fractal.

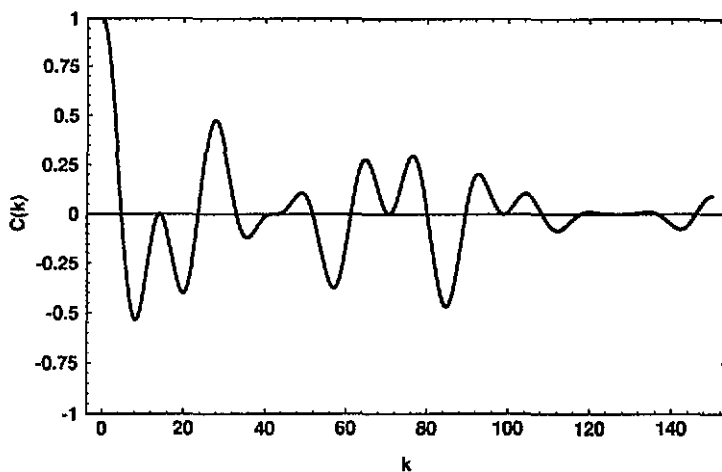


Figure 4. The Fourier transform of the Cantor set, defined by equation (4.1). Note the multiple zeros, which occur at k equal to $\pi/2$ multiplied by a power of 3.

5. Summary and discussion

The dimension of the fractal, while it appears repeatedly throughout the calculation (equations (2.12), (2.19), (2.24), (3.16) and (4.8)), gives only an outline of the full structure of the various quantities associated with the Cantor set. The potential contains, in addition to the expected power law behaviour, small oscillations in the logarithm of the distance from the fractal, together with a Taylor series. The moments of the distribution also have an oscillatory structure, which is only evident for $n \gtrsim 100$. The Fourier transform of the distribution is an entire function, and can be written as an infinite product of cosines. It does not tend to zero for large k , but follows a power law related to the dimension if averaged appropriately.

The methods used in this analysis could readily be generalized to include all distributions derivable from similarity transformations, such as uniform distributions on higher dimensional fractals (von Koch snowflake, Menger sponge, and so on) or *non-uniform multifractal distributions*, for example the *binomial distribution* on the Cantor set defined by

$$C_p(x) = 3[pC_p(3x - 1) + (1 - p)C_p(3x + 1)] \quad (5.1)$$

which reduces to the uniform case when $p = 1/2$. This may be of particular interest since the charge distributions on a fractal conducting surface have this kind of structure, as argued by Evertsz and Mandelbrot [6].

Acknowledgments

The authors wish to thank Dr Michael Shlesinger, Dr John Mitchell and Dr Vic Kowalenko for helpful discussions and Mr A Logothetis for assistance with the numerical computations. One of us (CD) acknowledges the support of an Australian Postgraduate Research Award.

References

- [1] Cutler C D 1991 *J. Stat. Phys.* **62** 651, addendum 1991 *J. Stat. Phys.* **65** 417
- [2] Vassilicos J C and Hunt J C R 1991 *Proc. R. Soc. A* **435** 505
- [3] Avron J E and Simon B 1981 *Phys. Rev. Lett.* **46** 1166
- [4] Silaev P K, Tyurin E N and Khrustalev O A 1991 *Teor. Mat. Fiz.* **89** 73 (Russian), translated in 1992 *Theor. Math. Phys.* **89** 1064
- [5] Taylor S J 1986 *Math. Proc. Camb. Phil. Soc.* **100** 383
- [6] Evertsz C J G and Mandelbrot B B 1992 *J. Phys. A: Math. Gen.* **25** 1781
- [7] Bessis D, Geronimo J S and Moussa P 1984 *J. Stat. Phys.* **34** 75
- [8] Landkof N S 1972 *Foundations of Modern Potential Theory* English edn (Berlin: Springer)
- [9] Berry M V 1979 *J. Phys. A: Math. Gen.* **12** 781
- [10] Sapoval B, Gobron T and Margolina A 1991 *Phys. Rev. Lett.* **67** 2974
- [11] Mandelbrot B B 1977 *The Fractal Geometry of Nature* (New York: Freeman)
- [12] Falconer K 1990 *Fractal Geometry and Its Applications* (Chichester: Wiley)
- [13] Dettmann C P and Frankel N E *Preprint* UM-P-92/67 University of Melbourne
- [14] Oberhettinger F 1974 *Tables of Mellin Transforms* (Berlin: Springer)
- [15] Hughes B D, Montroll E W and Shlesinger M F 1981 *Proc. Natl Acad. Sci. (USA)* **78** 3287; 1982 *J. Stat. Phys.* **28** 111; 1983 *J. Stat. Phys.* **30** 273
- [16] Hille F and Tamarkin J D 1929 *Am. Math. Mon.* **36** 255